Preliminary Characterization of Light Harvesting in *E. coli* DNA Photolyase

Allison A. Henry, Ralph Jimenez, Denise Hanway, and Floyd E. Romesberg*[a]

E. coli *DNA photolyase is a monomeric light-harvesting enzyme that utilizes a methenyltetrahydrofolate (MTHF) antenna cofactor to harvest light energy for the repair of thymine dimers in DNA. For this purpose, the enzyme evolved to bind the cofactor and red-shift its absorption maximum by 25 nm. Using the crystal structure as a guide, we mutated each protein residue that contacts the cofactor in an effort to identify the interactions responsible for this selective stabilization of the cofactor's excited state. Hydrogen bonding, packing, and electrostatic interactions were examined. Remarkably, a single residue, Glu109, appears to play an important, if not exclusive, role in inducing the observed red-shift. Thus, this protein, the simplest light-harvesting system known, appears to have evolved a remarkably simple mechanism to tune the photophysical properties of the antenna cofactor appropriately for biological function.*

Introduction

DNA photolyases are soluble enzymes that repair UV-light-induced DNA lesions, including the cyclobutane pyrimidine dimer (CPD) and the (6–4) photoproduct.[1] These enzymes have high sequence homology to the blue-light photoreceptor proteins of plants, though these are functionally divergent, and the DNA photolyases are themselves represented in many prokaryotic and eukaryotic organisms.[2] The CPD photolyase of *E. coli* (PL) is a monomeric protein that noncovalently binds two chromophoric cofactors: methenyltetrahydrofolylpolyglutamate (MTHF) and flavin adenine dinucleotide (FAD). Previous biological and physical studies of this enzyme by Sancar and Jorns elucidated its photoreactivation mechanism.[3–5] The MTHF antenna cofactor absorbs near-UV light and transfers this energy to the redox-active FAD cofactor by a Foerster-type mechanism.[6] In the active site of the holoenzyme, the first excited singlet state of $FADH_2$ transfers an electron to the CPD substrate, generating a labile radical anion that undergoes ring opening.

One of the most important but least understood aspects of PL-mediated DNA damage repair is how the MTHF binding site is able to tune the MTHF cofactor so that it can function as an antenna. In aqueous solution, MTHF absorbs light maximally at 358 nm. At this wavelength, the flux of solar radiation is lower than it is at longer wavelengths; so, to efficiently utilize MTHF as a light antenna, PL induces a 25 nm red-shift in the absorption maximum of the chromophore (to 383 nm) upon binding. This greater than 5 kcal mol^{-1} decrease in transition energy must result from protein-mediated stabilization of the excited state and/or destabilization of the ground state of MTHF. The specific protein–cofactor interactions that cause this significant and functionally critical red-shift are unknown, although they must include structural, electrostatic, dipolar, and hydrogen-bonding (H-bonding) contributions.

The crystal structure of PL at 2.3 Å resolution, solved in 1995,[7] reveals several interactions that might contribute to the red-shift. The structure shows the MTHF pteridine ring system in a surprisingly shallow and solvent-exposed binding site formed by H44, N108, E109, C292, and L375 (Scheme 1). Both the side-chain oxygen and the main-chain nitrogen of

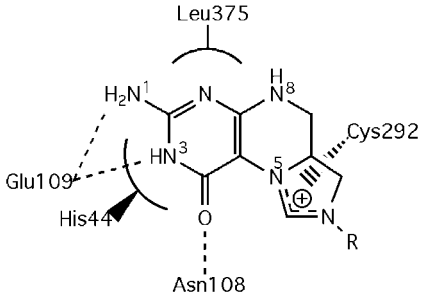

Scheme 1. *Schematic representation of MTHF in its PL binding site. R = N-(p-aminobenzoyl)polyglutamate.*

N108 are within H-bonding distance of the pteridine exocyclic oxygen, while the side chain of E109 is positioned to participate in two H-bonds donated from N^1 and N^3. The main-chain oxygen of C292 is only 3.1 Å away from N^{10}, which shares the delocalized positive charge with N^5. The pteridine is also packed between H44, in the vicinity of N^3, and L375 from the opposite side. To determine which of these interactions have been evolved to tune the antenna cofactor's absorption spectrum, we undertook a site-directed mutagenesis study. Each residue that interacts with the chromophoric moiety of MTHF was changed to alter the electrostatics, polarity, packing, and

[a] *A. A. Henry, Dr. R. Jimenez, D. Hanway, Prof. F. E. Romesberg*
Department of Chemistry, The Scripps Research Institute
10550 N. Torrey Pines Road, La Jolla, CA 92037 (USA)
Fax: (+1) 858-784-7472
E-mail: floyd@scripps.edu

Supporting information for this article is available on the WWW under http://www.chembiochem.org or from the author.

  DOI: 10.1002/cbic.200400013

H-bonding of the antenna cofactor binding site. The light-harvesting properties of the resultant mutant proteins were characterized by steady-state and femtosecond time-resolved spectroscopy.

Results and Discussion

Polarity-induced red-shift

To determine the potential contribution of bulk polarity to the red-shift of MTHF observed upon binding to the enzyme, UV/Vis absorption spectra were recorded for MTHF in aqueous buffer containing increasing amounts of methanol (Figure 1). The chromophore's absorption maximum shifts to the red by approximately 6 nm as the dielectric constant decreases from 78.5 to 32.6. This change in transition energy is significantly smaller than that observed upon binding to PL, and this result implies that nonspecific polarity effects within the MTHF binding site cannot be solely responsible for the observed red-shift. Thus, specific protein–cofactor interactions were examined.

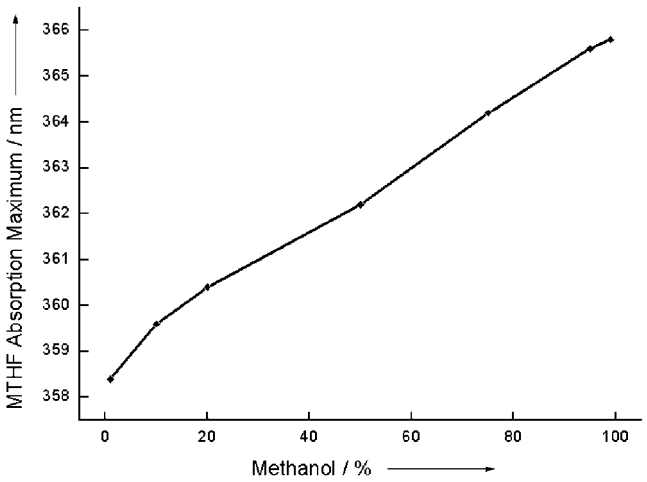

Figure 1. *MTHF in citrate buffer with varying percentages of methanol.*

Protein–cofactor interactions

Based on the crystal structure of PL, it appears that four of the five residues in the MTHF binding site that contact the pteridine ring system of the MTHF cofactor interact with the ground state of MTHF through their side chains.[7] There is no crystallographic evidence that the side chain of C292 interacts with the ground state of MTHF, only its main-chain oxygen; however, this does not preclude the possibility that this side chain has a role in stabilization of the excited state of MTHF. To determine which residues contribute to the observed red-shift, the side chain of each was changed by site-directed mutagenesis. Asn108, the side-chain and main-chain nitrogen atoms of which are within H-bonding distance of the pteridine exocyclic oxygen, was mutated to Leu. This substitution is isostructural but removes the H-bonding interaction involving the side chain. Glu109, the side chain of which shares H-bonds with N^1 and N^3 of the pteridine, was mutated to Asp or Gln. These mutations alter the structural or electronic properties of the two protein–cofactor H-bonds. Cys292, which appears to interact electrostatically with the N^5-to-N^{10} delocalized positive charge of MTHF through its main-chain oxygen, was mutated to Ser in order to probe this potential contribution to excited-state stabilization. Mutation of H44 to Phe allows the stacking interaction to be retained while significantly reducing polarity. Leu375 was substituted by both His and Phe to introduce polar and nonpolar aromatic interactions in place of aliphatic packing. In this manner, each of the direct interactions between the protein and the cofactor can be examined, and the specific contributions of H-bonding, packing, and electrostatics to the enzyme's light-harvesting properties may be determined.

Mutation of the MTHF binding site clearly affects the apparent binding affinity of the enzyme for the antenna cofactor, as judged by the loss of MTHF upon purification of the wild-type (wt) and mutant proteins. The UV/Vis spectra shown in Figure 2 confirm the expected form of the isolated proteins,

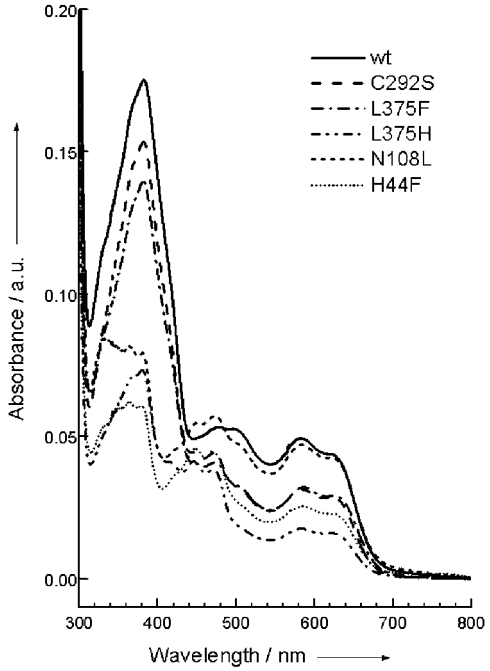

Figure 2. *UV/Vis spectra of purified wt and mutant proteins.*

with substoichiometric MTHF and stoichiometric FAD in its neutral radical semiquinone oxidation state ($FADH^{\bullet}$).[5] The absorption band centered at 580 nm is due to $FADH^{\bullet}$ ($\varepsilon_{580} = 4.8 \times 10^3\ M^{-1}cm^{-1}$)[8] and that at 443 nm is due to FAD_{ox} ($\varepsilon_{443} = 11.2 \times 10^3\ M^{-1}cm^{-1}$).[5] The absorption band centered at 380 nm represents a sum of contributions from MTHF ($\varepsilon_{380} = 25.9 \times 10^3\ M^{-1}cm^{-1}$),[5] $FADH^{\bullet}$ ($\varepsilon_{380} = 6.0 \times 10^3\ M^{-1}cm^{-1}$),[5] and FAD_{ox} ($\varepsilon_{380} = 11.0 \times 10^3\ M^{-1}cm^{-1}$),[5] but it is dominated by MTHF by virtue of its larger extinction coefficient. The differences in the spectra indicate only different amounts of $FADH^{\bullet}$, FAD_{ox}, and MTHF in the various protein samples. The mutants L375F and C292S appear to bind MTHF with affinity similar to wt, as dem-

onstrated by the approximately equal amount of cofactor that was retained throughout purification. L375H appears to bind MTHF somewhat more weakly than wt. In contrast, H44F, N108L, E109D, and E109Q retain no MTHF at all upon purification. However, the H44F and N108L mutant proteins were able to bind and retain MTHF under normal reconstitution conditions (see below), whereas the E109 mutants were unable to bind the cofactor under any conditions examined. Though this is obviously a qualitative determination of MTHF binding, it nonetheless clearly demonstrates that mutation of the MTHF binding site affects binding of the ground state of the antenna cofactor.

To determine the effect of each mutation on the spectral profile of MTHF, steady-state UV/Vis absorption and fluorescence emission spectra were obtained for each MTHF-reconstituted protein. The large absorption red-shift characteristic of wt protein-bound MTHF is conserved in each mutant protein, as the absorption maxima vary within a range of only 2 nm (Figure 3 and Table 1). The only spectral differences are attributed to small amounts of FAD_{ox} (see above). The emission spectra show little variation in position and shape at the high frequency side, but all of the mutants have spectra that are broadened to the red (Figure 4 and Table 1). This observation is also attributed to the presence of FAD_{ox}, for which the wavelength of maximum emission is 521 nm.[5] Apparently, none of the interactions mediated by the side chains of H44, N108, C292, or L375 contribute to selective stabilization of the excited state of MTHF.

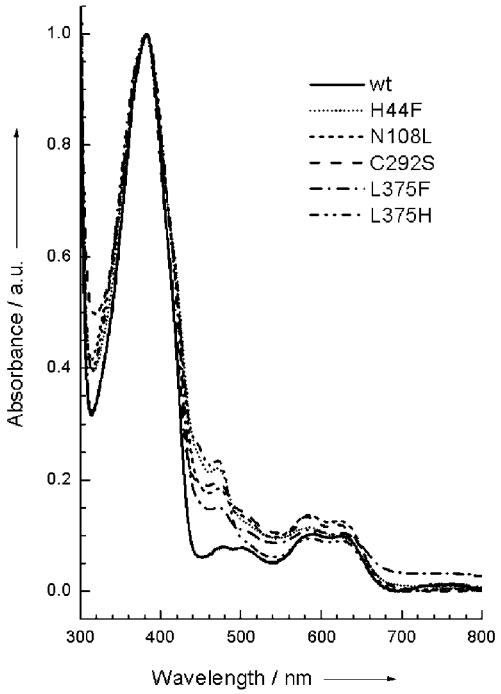

Figure 3. *UV/Vis spectra of MTHF-reconstituted wt and mutant proteins.*

Table 1. *Spectral data for wild-type and mutant-bound MTHF.*[a]

Mutant	λ_{max} (abs)	λ_{max} (em)	Stokes shift [cm^{-1}]	k_{et} [s^{-1}]
wt	383	470[b]	4974	5.4×10^9
H44F	381	484[b]	5906	4.8×10^9
N108L	383	481[b]	5805	7.5×10^9
C292S	382	480[c]	5765	6.2×10^9
L375F	383	474[b]	5174	3.4×10^9
L375H	381	481[b]	5764	5.5×10^9
MTHF(aq.)	358	470[b]	6638	n.a.[d]

[a] See text for experimental details. [b] $\lambda_{ex}=370$ nm. [c] $\lambda_{ex}=375$ nm. [d] Not applicable.

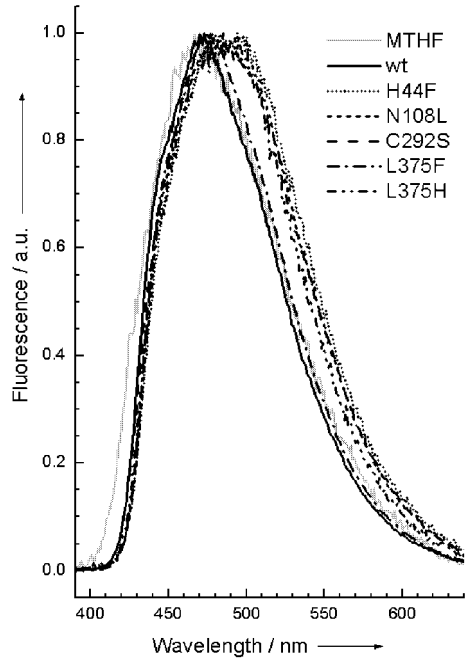

Figure 4. *Fluorescence emission spectra of MTHF-reconstituted wt and mutant proteins.*

Interchromophore energy transfer

Although there were no significant changes in the absorption or emission profile of enzyme-bound MTHF with mutation of its binding site, the presence of small amounts of FAD_{ox} interfered with the steady-state spectra of the E-MTHF-$FADH^{\bullet}$ form of the enzymes and might have masked small changes in the spectra of the antenna cofactor. Thus, to independently probe the light-harvesting properties of the PL mutants, we measured the interchromophore energy-transfer rate for each protein in the physiologically relevant form, E-MTHF-$FADH_2$.[9] The second harmonic of a cavity-dumped Ti:sapphire femtosecond regenerative amplifier was used to generate pump and probe pulses for single-color (406 nm) transient absorption experiments. UV/Vis spectra were recorded before and after laser scanning and indicated, by comparison of the ratios of absorbance at 360 nm and 385 nm, that: 1) no measurable dissociation of the MTHF cofactor occurred during the experiments, and 2) the extent of photodecomposition of the MTHF cofactor ranged from 1% to 10%, averaging 6% and depending only on the number of scans required for enhancing the signal-to-noise ratio. The raw transient absorption data were normalized

and fitted to a sum of exponential terms convoluted with the pulse width that yielded the time constants for MTHF ground-state repopulation in the various proteins (Figure 5, Table 1,

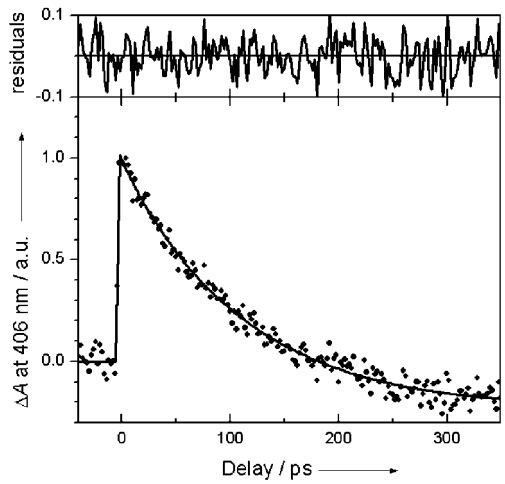

Figure 5. *Representative transient absorption spectrum of MTHF-reconstituted wt PL with nonlinear least-squares fit and residuals.*

and Supporting Information). The minor fast component (approximately 30 ps) is attributed to resonant energy transfer to $FADH^{\bullet}$, and the minor slow component (1.4 ns), which causes the signal to become negative, is attributed to absorption of the probe beam by a transiently formed excited state of the flavin.[10] The major component (>80%) of each fit, representing both resonant energy transfer to $FADH_2$ and the radiative transition, has an associated time constant of approximately 120 ps. The rate constant for energy transfer was determined from this parameter by using the previously determined rate constant for the cofactor's radiative transition, $2.8\times10^9\ s^{-1}$ (Table 1).[10] Mutant L375F exhibited the least efficient interchromophore energy transfer while mutant N108L displayed the most efficient interchromophore energy transfer. However, overall the rates of resonant energy transfer were found to vary by only 2.2-fold (Table 1).

The greatest effect of mutation of the MTHF binding site was the abrogation of cofactor binding that resulted from even minor perturbations at Glu109. In each of the other five mutants, it is interesting that mutation had such minor effects on the antenna cofactor's absorption and interchromophore energy transfer. The aromatic and aliphatic packing interactions of His44 and Leu375 do not appear to be involved in red-shifting the chromophore. This implies that geometric distortion of MTHF is not critical for the red-shift and that these residues do not play a role in positioning the chromophore appropriately for energy transfer to the FAD cofactor. The invariance of the absorption maximum to mutation at Asn108 and Cys292 implies that if these residues contribute to the decrease in transition energy, it is through their main-chain atoms. Because each residue that contacts the pteridine of MTHF was examined, the results allow for two possible interpretations: that the red-shift is induced by main-chain–cofactor interactions, or that Glu109 is of paramount importance not only to MTHF binding, but also to stabilizing its excited state.

Contributions of the Glu109 side chain and protein backbone to the red-shift

Main-chain amide groups contain H-bond donor and acceptor functionalities and have permanent dipoles that may interact differentially with the MTHF ground and excited states, thus affecting the chromophore's transition frequency. The crystal structure of PL shows two close contacts between main-chain atoms and the cofactor: the peptide oxygen of Cys292 is 3.1 Å from N^{10} of the cofactor, and the peptide nitrogen of Asn108 is 2.7 Å from the pteridine exocyclic oxygen.[7] Electrostatic interactions in the former case and a H-bond in the latter case may selectively stabilize the MTHF excited state and contribute to the observed red-shift.

Alternatively, several arguments support a role for Glu109 in the red-shift of the antenna cofactor. In the crystal structure, two H-bonds are observed between the Glu109 side chain and atoms N^1 and N^3 of the pteridine ring system (Scheme 1). As discussed above, this interaction is required for cofactor binding, and does not tolerate even small electronic or structural perturbations. Though this precludes direct evaluation of the Glu109 side chain's contribution to the red-shift of MTHF by the methods described above, previous molecular-orbital calculations predicted that this residue might significantly stabilize the MTHF excited state, as well as the ground state. These calculations suggest that, upon excitation, charge migrates away from N^1 and N^3 of the pteridine, where an appropriately positioned negative charge, such as the carboxylate of the Glu109 side chain, would stabilize the excited state of MTHF relative to its ground state.[11]

Because mutation of Glu109 abrogates MTHF binding, and because the protein backbone cannot easily be altered, it is difficult to experimentally determine the relative contributions of these groups to the selective stabilization of the MTHF excited state. However, FTIR may be used to evaluate the contributions of these same functionalities to MTHF ground-state binding, as the vibrations of any group that strongly interacts with the cofactor will differ between the bound (E-MTHF-$FADH^{\bullet}$) and unbound (E-$FADH^{\bullet}$) states of the protein. These differences will be made manifest as negative and positive peaks in the IR difference spectrum, the negative features corresponding to the lost absorptions of the unbound state and the positive features corresponding to the absorptions gained in the bound state. The frequencies observed for these features may be used to identify the functional groups that interact strongly with the added MTHF.

We measured the FTIR spectra of wt PL in both MTHF-depleted and MTHF-reconstituted forms under standard PL-handling conditions (see below). Both the unreconstituted sample and the reconstituted sample were incubated under identical conditions, except for the presence of MTHF in the latter, and both were passed over a desalting column and concentrated immediately prior to the FTIR measurements. Thus, the only difference in sample composition should be the state

of the protein with respect to MTHF. In the difference spectrum (Figure 6), the positive band centered at 1608 cm^{-1} probably results from MTHF absorption, as do the overlapping absorptions at frequencies lower than 1500 cm^{-1}. However, there is a prominent negative band at 1548 cm^{-1} and a prominent positive band at 1699 cm^{-1}. The frequency of the positive absorption is too high to correspond to an amide vibration, and this implies that backbone amide groups do not strongly interact with the cofactor in the ground state. Furthermore, in the absence of significant conformational rearrangement, this will also be true for MTHF in the excited state. Instead, these spectral features are consistent with the loss of a COO^- asymmetric stretching absorption and the gain of an absorption by protonated or hydrogen-bonded COO^- upon reconstitution of wt PL with MTHF.[12] Thus, this result suggests that, in the ground state, the MTHF cofactor interacts strongly with the carboxylate of either an Asp or a Glu side chain and not the protein backbone. This observation strengthens the conclusion that Glu109 plays a central role in MTHF binding, as discussed above. Although it is difficult to precisely interpret, the frequency of the positive peak in the difference spectrum (1699 cm^{-1}) is lower than what would be expected for a fully protonated carboxylic acid moiety (often observed at up to 1750 cm^{-1});[13] this implies that the Glu109 side chain–MTHF H-bond may not be optimized in the ground state. If this is the case, the H-bond may be strengthened in the excited state, leading to its selective stabilization and induction of the observed red-shift. This hypothesis is consistent with the increase in positive charge at the N^1/N^3 H-bond donors predicted to characterize the MTHF excited state.[11] Thus, Glu109 might not only be required for antenna cofactor binding, but also for the selective stabilization of the MTHF excited state and thereby the absorption red-shift that is important for the biological function of the enzyme.

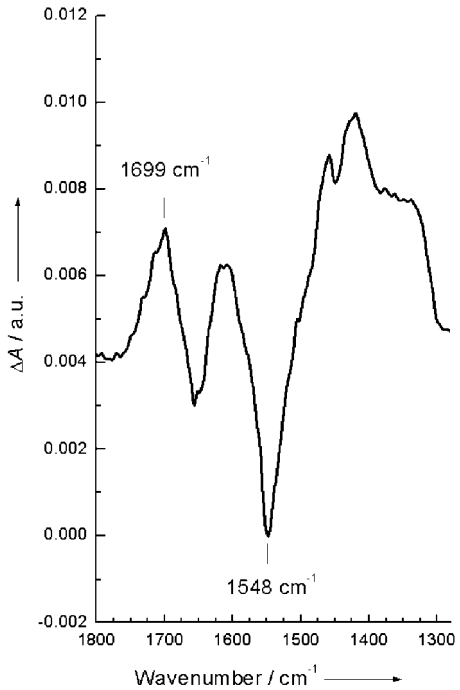

Figure 6. *FTIR difference spectrum of wt PL with and without bound MTHF.*

Conclusion

Proteins have evolved to bind cofactors or substrates and manipulate their physical properties appropriately for biological function. This is accomplished by differential stabilization of the molecule's ground state and excited or transition state. For light-harvesting proteins, for which the wavelength of light absorption is critical, the stability of the ground and excited states of the chromophore must be manipulated so that their difference in energy is matched with the energy of the available light. The electronic energy gap of MTHF is too large to efficiently absorb photons of visible light and efficiently function as a light-harvesting antenna. Therefore, in order to employ MTHF in this capacity, photolyase must selectively stabilize its excited state relative to its ground state.

The data presented above clearly indicate that the residues seen to contact the MTHF cofactor in the crystal structure, especially Glu109, are critical for ground-state binding, although more detailed studies are required to quantify the contributions of each residue. The steady-state and time-resolved data also clearly demonstrate that each direct interaction, other than with Glu109, does not contribute to the functionally critical red-shift. The FTIR data, along with these results, imply that PL has evolved to tune the antenna cofactor by positioning it, with respect to Glu109, in a manner that does stabilize the ground state but stabilizes the excited state to an even greater extent. Specific positioning of the cofactor, relative to the Glu109 side chain, is consistent with the complete loss of cofactor binding that accompanies even the most conservative mutation of this residue to Asp. Thus, this protein, the simplest light-harvesting system known, appears to have evolved a remarkably simple mechanism to tune the photophysical properties of the antenna cofactor appropriately for its biological function.

Experimental Section

General methods: All antibiotics and molecular biology reagents were purchased from Sigma, except DTT and IPTG, which were purchased from Promega. M15(pRep4) cells and the hyperexpression vector for *E. coli* DNA photolyase, pEphr, were kindly provided by Dr. Gerald Richter (Technical University of Munich). Site-specific mutations to the MTHF binding site were made with the QuikChange Site-Directed Mutagenesis Kit (Stratagene). The appropriate overlapping mutagenic primers with silent restriction sites were obtained from Operon. The mutations were confirmed by sequencing. All buffers used in protein purification were degassed with nitrogen, and DTT was added immediately prior to use. Blue Sepharose 6 Fast Flow and Sephacryl 300 HR column media were purchased from Amersham Biosciences; Bio-Gel P-6 DG Desalting Gel was purchased from Bio-Rad Laboratories.

Protein expression and purification: PL wt and mutant proteins were hyperexpressed and purified according to a slightly modified literature procedure.[14] M15(pRep4) cells harboring wild-type or

mutant pEphr were cultivated in baffled flasks containing LB medium (2 L) supplemented with kanamycin (15 μg mL^{-1}) and ampicillin (100 μg mL^{-1}). The cultures were incubated with shaking at 25 °C until an OD_{600} of 0.8 was reached. IPTG was added to a final concentration of 1 mM, and incubation with shaking was continued until the culture reached stationary phase. Cells were harvested by centrifugation (10000 *g*, 10 min, 4 °C) and the pellet (25 g from 10 L) was thawed at 4 °C in lysis buffer (50 mM Tris-HCl, pH 7.5, 100 mM NaCl, 10% (*w*/*v*) sucrose, and 10 mM DTT). Cells were lysed by sonication and centrifuged to remove cell debris (48000 *g*, 1 h, 4 °C). The supernatant was combined with $(NH_4)_2SO_4$ (0.43 g mL^{-1}), centrifuged (48000 *g*, 1 h, 4 °C), and the resultant pellet was dissolved in buffer (50 mM Tris-HCl, pH 7.5, 1 mM EDTA, 0.1 M KCl, 20% (*v*/*v*) glycerol, and 2 mM DTT) and desalted by dialysis against the same buffer. The protein solution was loaded onto a Blue Sepharose 6 Fast Flow column (50 mL), washed with low-salt buffer (50 mM Tris, pH 7.5, 1 mM EDTA, 0.1 M KCl, 20% (*v*/*v*) glycerol, and 1 mM DTT) and eluted with high-salt buffer (50 mM Tris, pH 7.5, 1 mM EDTA, 2 M KCl, 20% (*v*/*v*) glycerol, and 10 mM DTT). Blue fractions were combined, concentrated with a Centriplus YM-30 device (Amicon), and loaded onto a Sephacryl 300 HR column (40 mL) equilibrated and run in phosphate buffer (67 mM potassium phosphate, 1 mM EDTA, 10% (*v*/*v*) glycerol, and 2 mM DTT). Blue fractions were combined with $(NH_4)_2SO_4$ (0.43 g mL^{-1}), centrifuged (48000 *g*, 1 h, 4 °C), and the pellets were dissolved in storage buffer (50 mM Tris-HCl, pH 7.5, 50 mM NaCl, 1 mM EDTA, 50% (*v*/*v*) glycerol, and 10 mM DTT). The protein solution was desalted by dialysis against storage buffer and stored at −80 °C. The protein concentration was determined by visible-light absorbance due to FADH$^{\bullet}$ ($\varepsilon_{580} = 4.8 \times 10^3$ M^{-1} cm^{-1}).[8]

Reconstitution and photoreduction: 5,10-methenyltetrahydrofolate was synthesized from 5-formyltetrahydrofolic acid by a previously reported method and stored at −20 °C in HCl (0.01 N).[15] MTHF-depleted purified protein was reconstituted by a method based on a literature procedure.[16] MTHF (20 mM) stock was diluted tenfold in citrate buffer (50 mM citrate, pH 6, 50 mM NaCl, 1 mM EDTA, 10 mM DTT) and added, in twofold molar excess, to the enzyme in storage buffer. The solution was incubated at 0 °C for 30 min and passed over a Bio-Gel P-6 DG desalting column (4 mL) run in enzyme storage buffer with reduced glycerol content (Buffer E) (50 mM Tris-HCl, pH 7.5, 50 mM NaCl, 1 mM EDTA, 20% (*v*/*v*) glycerol, and 10 mM DTT). Binding of MTHF to the protein was confirmed by the UV/Vis spectrum of the sample, indicated by an increase in absorbance around 383 nm. To convert enzyme-bound FAD_{ox} and FADH$^{\bullet}$ to $FADH_2$, samples were combined with additional fresh DTT (to a final concentration of 2 mM), degassed under positive pressure with argon, and transferred anaerobically to the spin cell for pump–probe analysis. Samples were photoreduced in the spin cell by illumination with 532 nm (5 mW) laser light for 10–20 min. Photoreduction was confirmed by a loss of absorbance at wavelengths longer than 400 nm in the UV/Vis spectrum.[5,17]

Steady-state spectroscopy: UV/Vis spectra were collected for 30 μM samples in Buffer E with a Cary 300 Bio UV/Vis spectrophotometer, in steps of 0.2 nm with an averaging time of 0.3 s at 25 °C. Fluorescence spectra were collected for 250 μM samples in Buffer E with a SPEX Fluorolog fluorescence spectrophotometer; the excitation wavelength was 370 nm or 375 nm and its bandwidth 2 nm. Emission was scanned at 25 °C in 1 nm steps over 1 s with a bandwidth of 2 nm. The raw data were fitted to a log normal distribution to determine the wavelength of maximum emission and to quantify the asymmetry of each spectrum.[18]

Transient absorption spectroscopy: A fused silica spin cell was used with a 250 μm Teflon spacer; this enabled the use of 200 μL of a 0.5 mM protein solution in Buffer E, giving optical densities of approximately 0.2 at 400 nm. The pump and probe pulses, both 406 nm, were generated by means of a cavity-dumped Ti:sapphire oscillator pumped by 3 W of 532 nm light from a Spectra Physics Millenia solid-state laser. The repetition rate was set to 5 kHz, and the pulse energy was 20 nJ; this gave a chopped pump beam power of 50 mW and a probe beam power of 6 mW. The spatially overlapped pump and probe beams were focused by means of a lens onto the spinning sample (4000 rpm). A silicon photodiode was used to detect the amount of the probe beam exiting the sample cell. The time delay of the probe pulse, increasing in steps of 2 ps over a total of 400 ps, was set by a mirror mounted on a stage under electronic control. Typically, 20 complete scans were averaged to yield the raw kinetic data. The raw data were normalized and fitted with a nonlinear least-squares function, including a Gaussian convolution for the instrument response (negligible due to the ultrafast incident pulse of 25 fs). This fit yielded the observed time constants for MTHF ground-state repopulation, which were converted to the rate constant for energy transfer by a simple calculation based on the relationship between the observed time constant (τ_{obs}), the rate constant for the radiative transition (k_{rad}), and the rate constant for energy transfer (k_{et}): $1/\tau_{obs} = k_{rad} + k_{et}$.

FTIR spectroscopy: FTIR spectra were collected with a Bruker Equinox 55 spectrometer equipped with a DTGS detector and continuously flushed with dry nitrogen. Spectra were constructed from 128 scans, two orders of zero filling, and Blackman–Harris three-term apodization. All protein samples were measured at a concentration of 600 μM in Buffer E. Samples were loaded into a modified liquid transmission cell with 25 mm diameter CaF_2 windows (Pike Technologies, Madison, WI) and a 15 μm Teflon spacer. Spectral subtraction was performed by using the Bruker OPUS software with a subtraction factor close to 1.

Abbreviations

MTHF, 1,5-methenyltetrahydrofolate; FAD, flavin adenine dinucleotide; FAD_{ox}, FAD in its fully oxidized state; FADH$^{\bullet}$, FAD in its semireduced state; $FADH_2$, FAD in its fully reduced state; PL, *E. coli* DNA photolyase; DTT, dithiothreitol; IPTG, isopropyl-β-thio-D-galactopyranoside

Acknowledgements

Molecular graphics images were produced by using the UCSF Chimera package from the Computer Graphics Laboratory, University of California, San Francisco (supported by NIH P41 RR-01081). We thank Dr. Julius Rebek for access to the SPEX Fluorolog, Dr. Gerald Richter for the photolyase expression system, and The Skaggs Institute of Chemical Biology for funding.

Keywords: chromophores · mutagenesis · photolyase · steady-state spectroscopy · time-resolved spectroscopy

[1] T. Carell, L. T. Burgdorf, L. M. Kundu, M. Cichon, *Curr. Opin. Chem. Biol.* **2001**, *5*, 491–498.
[2] S. Kanai, R. Kikuno, H. Toho, H. Ryo, T. Todo, *J. Mol. Evol.* **1997**, *45*, 535–548.
[3] A. Sancar, *Biochemistry* **1994**, *33*, 2–9.

[4] L. P. Chanderkar, M. S. Jorns, *Biochemistry* **1991**, *30*, 745 – 754.
[5] M. S. Jorns, B. Wang, S. P. Jordan, L. P. Chanderkar, *Biochemistry* **1990**, *29*, 552 – 561.
[6] T. Foerster, *Disc. Farad. Soc.* **1959**, *27*, 1.
[7] H.-W. Park, S.-T. Kim, A. Sancar, J. Deisenhofer, *Science* **1995**, *268*, 1866 – 1872.
[8] B. Wang, M. S. Jorns, *Biochemistry* **1989**, *28*, 1148 – 1152.
[9] G. Payne, P. F. Heelis, B. R. Rohrs, A. Sancar, *Biochemistry* **1987**, *26*, 7121 – 7127.
[10] S.-T. Kim, P. F. Heelis, T. Okamura, Y. Hirata, N. Mataga, A. Sancar, *Biochemistry* **1991**, *30*, 11 262 – 11 270.
[11] P. F. Heelis, *J. Photochem. Photobiol. B* **1997**, *38*, 31 – 34.
[12] T. Noguchi, M. Sugiura, *Biochemistry* **2001**, *40*, 1497 – 1502.
[13] P. Hellwig, J. Behr, C. Ostermeier, O.-M. H. Richter, U. Pfitzner, A. Odenwald, B. Ludwig, H. Michel, W. Maentele, *Biochemistry* **1998**, *37*, 7390 – 7399.
[14] C. W. M. Kay, R. Feicht, K. Schultz, P. Sadewater, A. Sancar, A. Bacher, K. Moebius, G. Richter, S. Weber, *Biochemistry* **1999**, *38*, 16 740 – 16 748.
[15] J. C. Rabinowitz, *Methods Enzymol.* **1963**, *6*, 814 – 815.
[16] S. Hamm-Alvarez, A. Sancar, K. V. Rajagopalan, *J. Biol. Chem.* **1989**, *264*, 9649 – 9656.
[17] P. F. Heelis, A. Sancar, *Biochemistry* **1986**, *25*, 8163 – 8166.
[18] M. Maroncelli, G. R. Fleming, *J. Chem. Phys.* **1987**, *86*, 6221 – 6239.

Received: January 16, 2004

